

UR-1383, ER-40685-832

November 1994

PARITY VIOLATION IN TOP QUARK PAIR PRODUCTION AT THE FERMILAB TEVATRON COLLIDER

CHUNG KAO¹

*Department of Physics and Astronomy, University of Rochester
Rochester, NY 14627, USA*

Abstract

The leading weak corrections to the production of top quark pairs via $q\bar{q} \rightarrow t\bar{t}$ in $p\bar{p}$ collisions are evaluated. The chromo-anapole form factor of the top quark and effects of parity violation are studied in the Standard Model (SM) and the Minimal Supersymmetric Model (MSSM). The parity violation effect in $q\bar{q} \rightarrow g \rightarrow t\bar{t}$ from the SM weak corrections is found to be very small. In the MSSM, the effects of parity violation can be enhanced for $\tan\beta \equiv v_2/v_1 > \sqrt{m_t/m_b}$.

¹Internet Address: KAO@URHEP.PAS.ROCHESTER.EDU

1. Introduction

In the Standard Model (SM) and some of its extensions, the Yukawa couplings of a fermion to elementary spin-0 bosons are proportional to the fermion mass. The top quark now appears to be very heavy [1, 2]; therefore, its Yukawa couplings are interestingly large. Many processes involving the top quark and the ‘Higgs bosons’ might provide opportunities to investigate physics of the electroweak symmetry breaking.

The QCD corrections [3]-[6] to the production rate of $q\bar{q} \rightarrow t\bar{t}$ are larger than the weak corrections [7]-[10]. However, the manifestation of parity violation in the electroweak interactions might produce effects unobtainable from QCD, which conserves both parity (P) and charge conjugation (C) symmetries. In the SM, the dominant decay mode of the top quark is $t \rightarrow W^+b$. Since the top quark appears to be so heavy, its lifetime is much shorter than the time needed to flip its spin [11]. The helicity of the top quark can be deduced from the energy distribution of the W ’s or the leptons in the W decays. It was recently suggested [10] that an asymmetry in the production rate of a right-handed top quark associated with a left-handed top antiquark ($t_R\bar{t}_L$) and $t_L\bar{t}_R$ can be a good observable of parity violation. This asymmetry from the SM weak corrections was found to be small.

In this paper, the leading weak corrections to $q\bar{q} \rightarrow g \rightarrow t\bar{t}$ are evaluated in the Minimal Supersymmetric Model (MSSM)² as well as in the SM. The

² Reviews for the MSSM can be found in [12]-[16]. Recent studies on the search for MSSM Higgs bosons are to be found in [17]-[21].

chromo-anapole form factor of the top quark is calculated to study effects of parity violation in top quark pair production at the Fermilab Tevatron, where $q\bar{q}$ annihilation dominates the production of $t\bar{t}$. Gluon fusion ($gg \rightarrow t\bar{t}$) will be the major source of SM top quark pairs at the Large Hadron Collider (LHC)³. Parity violation in $t\bar{t}$ production via $q\bar{q}$ annihilation and gluon fusion at the LHC is currently under investigation. The parity conserving corrections from QCD and QED do not affect the parity violating asymmetries; therefore, they are not included in our analysis.

2. The Top Quark Chromo-anapole Form Factor

In the SM, the $gt\bar{t}$ vertex gets one-loop weak corrections from the Higgs boson (H^0), the neutral and charged Nambu-Goldstone bosons (G^0, G^\pm), the Z boson (Z) and the W bosons (W^\pm). The Feynman diagrams are shown in Figure 1. In the 't Hooft-Feynman gauge, the weak interaction Lagrange density involving the top quark is

$$\begin{aligned}\mathcal{L}_I = & -\bar{t}\gamma^\mu(g_V - g_A\gamma_5)tZ_\mu \\ & -\frac{g}{2\sqrt{2}}[\bar{t}\gamma^\mu(1 - \gamma_5)bW_\mu^+ + \bar{b}\gamma^\mu(1 - \gamma_5)tW_\mu^-] \\ & -\frac{m_t}{v}\bar{t}tH^0 + i\frac{m_t}{v}\bar{t}\gamma_5tG^0 \\ & +\frac{m_t}{\sqrt{2}v}[\bar{t}(\lambda_s^G - \lambda_p^G\gamma_5)bG^+ + \bar{b}(\lambda_s^G + \lambda_p^G\gamma_5)tG^-]\end{aligned}\quad (1)$$

where $g_V = \frac{g}{4\cos\theta_W}[1 - \frac{8\sin^2\theta_W}{3}] \sim 0.08$, $g_A = \frac{g}{4\cos\theta_W} \sim 0.19$, $\lambda_s^G = 1 -$

³ It might be possible that some large new physics effects will appear in the process of $q\bar{q} \rightarrow t\bar{t}$ [22] and $gg \rightarrow t\bar{t}$ [23] at the LHC.

$\frac{m_b}{m_t}$, $\lambda_p^G = 1 + \frac{m_b}{m_t}$, v is the vacuum expectation value (VEV) of the Higgs doublet and θ_W is the Weinberg weak mixing angle. We take $V_{tb} = 1$ for simplicity. The quark mixing from the CKM matrix is not included; thus, CP is conserved.

In the Minimal Supersymmetric Model (MSSM), there are two Higgs doublets and five Higgs bosons: a pair of singly charged Higgs bosons, H^\pm ; two neutral CP-even Higgs bosons, H (heavier) and h (lighter); and a CP-odd Higgs boson, A . The Lagrange density involving the top quark and the Higgs bosons in the MSSM is

$$\begin{aligned}\mathcal{L}_I = & -\left[\frac{\sin \alpha}{\sin \beta}\right] \frac{m_t}{v} \bar{t} t H - \left[\frac{\cos \alpha}{\sin \beta}\right] \frac{m_t}{v} \bar{t} t h \\ & + i[\cot \beta] \frac{m_t}{v} \bar{t} \gamma_5 t A \\ & + \frac{m_t}{\sqrt{2}v} [\bar{t}(\lambda_s^H - \lambda_p^H \gamma_5) b H^+ + \bar{b}(\lambda_s^H + \lambda_p^H \gamma_5) t H^-]\end{aligned}\quad (2)$$

where $\tan \beta \equiv v_2/v_1$ is the ratio of the two Higgs doublet VEV's, $\lambda_s^H = \cot \beta + \frac{m_b}{m_t} \tan \beta$, $\lambda_p^H = \cot \beta - \frac{m_b}{m_t} \tan \beta$, and α is the mixing angle between the neutral CP-even Higgs bosons. At the tree level, all masses and couplings of Higgs bosons can be determined with only two independent parameters, which we choose to be $\tan \beta$ and the mass of the charged Higgs boson M_{H^\pm} . We have included one loop corrections from top and bottom Yukawa interactions to the Higgs masses and couplings using the effective potential [24]-[26]. For simplicity, we assume that all squarks have the same mass $m_Q = 1$ TeV; all neutralinos and charginos are very heavy; and there is no mixing between the top squarks \tilde{t}_L and \tilde{t}_R .

The 't Hooft-Feynman gauge is employed to evaluate the loop diagrams with $M_{G^0} = M_Z$ and $M_{G^+} = M_W$. We take $M_W = 80.22$ GeV, $M_Z = 91.187$ GeV, $m_b = 4.8$ GeV, $m_t = 170$ GeV and $\sin^2 \theta_W = 0.2319$. The updated parton distribution functions of CTEQ3L [27] are chosen to evaluate the cross section of $p\bar{p} \rightarrow t\bar{t} + X$ with $\Lambda = 0.177$ GeV and $Q^2 = \hat{s}$.

Let us write the $gt\bar{t}$ vertex as

$$-ig_s \bar{u}(p) T^a \Gamma^\mu v(q) \quad (3)$$

where g_s is the strong coupling, T^a are the $SU_C(3)$ matrices, $u(p)$ and $v(q)$ are the Dirac spinors of t and \bar{t} with outgoing momenta p and q . At the tree level, $\Gamma_0^\mu = \gamma^\mu$. The 1-loop vertex function can be expressed in terms of form factors [28]

$$\begin{aligned} \Gamma_1^\mu &= \gamma^\mu [A(k^2) - B(k^2)\gamma_5] \\ &+ (p-q)^\mu [C(k^2) - D(k^2)\gamma_5] \\ &+ (p+q)^\mu [E(k^2) - F(k^2)\gamma_5] \end{aligned} \quad (4)$$

where $k = p + q$, $k^2 = M_{t\bar{t}}^2 = \hat{s}$, and $M_{t\bar{t}}$ is the invariant mass of $t\bar{t}$. The conservation of vector current demands that $B(k^2) = -k^2 F(k^2)/(2m_t)$ and $E(k^2) = 0$. Applying the Gordon identities, we obtain

$$\begin{aligned} \Gamma_1^\mu &= F_1(k^2)\gamma_\mu - F_2(k^2)i\sigma^{\mu\nu}k_\nu \\ &+ a(k^2)\gamma_\nu\gamma_5(k^2 g^{\mu\nu} - k^\mu k^\nu) + d(k^2)i\sigma^{\mu\nu}k_\nu\gamma_5 \end{aligned} \quad (5)$$

Comparing both expressions for the Γ_1^μ , we obtain (1) $F_1(k^2) = A(k^2) + 2m_t C(k^2)$, $F_1(0) =$ the chromo-charge; (2) $F_2(k^2) = C(k^2)$, $F_2(0) =$ the

anomalous chromo-magnetic moment; (3) $a(k^2) = -B(k^2)/k^2 = F(k^2)/2m_t$, $a(0)$ = chromo-anapole moment; and (4) $d(k^2) = D(k^2)$, $d(0)$ = the chromo-electric dipole moment. The quark mixing from the CKM matrix is not included; therefore, the electric dipole form factor $D(k^2)$ is equal to zero in our analysis.

A nonzero anapole form factor generates signatures of parity violation. In the SM, the chromo-anapole form factor B_{SM} has contributions from the Z (B_Z), the W^+ (B_W), and the G^+ (B_G). Only the real parts of the form factors appear in the observables that we will discuss. Therefore, we present the real part of the form factor $B(k^2)$ in Figure 2 for every diagram and the SM total. Since the form factor $B(k^2)$ is proportional to $\hat{s} = M_{t\bar{t}}^2$, the parity violation effect will be greatly enhanced at higher energy. The Z boson contributes very little to the anapole form factor of the top quark since $2g_V g_A$ is small. In the 't Hooft-Feynman gauge, $|Re(B_G)|$ is larger than the full $|Re(B_{SM})|$, because the B_G and the B_W have opposite signs. The total B_{SM} appears to be small.

In the MSSM, the chromo-anapole form factor B_{MSSM} gets an additional contribution (B_H) from the charged Higgs boson. The form factor B_H is a function of M_{H^+} and $\tan \beta$. It is proportional to $\lambda^H = \lambda_s^H \lambda_p^H = \cot^2 \beta \{1 - [(m_b/m_t) \tan^2 \beta]^2\}$. For $M_{t\bar{t}}$ larger than about 400 GeV, if $\tan \beta > \sqrt{m_t/m_b}$, then $\lambda^H < 0$ and the B_H and the B_{SM} interfere constructively. On the other hand, if $\tan \beta < \sqrt{m_t/m_b}$, then the B_H and the B_{SM} interfere destructively.

When $M_{t\bar{t}}$ is close to the $2m_t$ threshold, the relative sign between the B_H and the B_{SM} is opposite to the relative sign for $M_{t\bar{t}}$ above 400 GeV. For $\tan\beta = \sqrt{m_t/m_b}$, B_H vanishes and the B_{MSSM} is equal to the B_{SM} . Figure 3 shows the form factor B_{MSSM} for various values of M_{H^+} and $\tan\beta$.

3. Asymmetries and Parity Violation

Let us define the cross section of the subprocess $q\bar{q} \rightarrow t\bar{t}$ in each helicity state of the $t\bar{t}$ as

$$\hat{\sigma}_{\lambda_1, \lambda_2} \equiv \hat{\sigma}(q\bar{q} \rightarrow t_{\lambda_1} \bar{t}_{\lambda_2}) \quad (6)$$

where $\lambda_{1,2}$ represents a right-handed (R) or a left-handed (L) helicity. At the tree level,

$$\begin{aligned} \hat{\sigma}_{LL}^{(0)} &= \hat{\sigma}_{RR}^{(0)} = \frac{4\pi\alpha_s^2\beta}{27\hat{s}^2}(2m_t^2) \\ \hat{\sigma}_{LR}^{(0)} &= \hat{\sigma}_{RL}^{(0)} = \frac{4\pi\alpha_s^2\beta}{27\hat{s}^2}(\hat{s}) \\ \hat{\sigma}^{(0)} &= \hat{\sigma}_{LL}^{(0)} + \hat{\sigma}_{RR}^{(0)} + \hat{\sigma}_{LR}^{(0)} + \hat{\sigma}_{RL}^{(0)} = \frac{8\pi\alpha_s^2\beta}{27\hat{s}}(1 + 2m_t/\hat{s}) \end{aligned} \quad (7)$$

where the cross section has been summed and averaged over spins and colors of the quarks in the initial state.

With one loop weak corrections, the cross section in each helicity state of $t\bar{t}$ is $\hat{\sigma}_{\lambda_1, \lambda_2} = \hat{\sigma}_{\lambda_1, \lambda_2}^{(0)} + \delta\hat{\sigma}_{\lambda_1, \lambda_2}$; where $\delta\hat{\sigma}_{\lambda_1, \lambda_2}$ is the contribution from weak corrections. The K -factor in each helicity state of the $t\bar{t}$ is defined as

$$K_{\lambda_1, \lambda_2} \equiv \frac{\hat{\sigma}_{\lambda_1, \lambda_2}}{\hat{\sigma}_{\lambda_1, \lambda_2}^{(0)}} = 1 + \frac{\delta\hat{\sigma}_{\lambda_1, \lambda_2}}{\hat{\sigma}_{\lambda_1, \lambda_2}^{(0)}} \quad (8)$$

These K -factors can be expressed in terms of the form factors:

$$\begin{aligned}
K_{LL} &= 1 + 2\text{Re}(A) - \beta^2 \hat{s} \text{Re}(C)/m_t + \beta \hat{s} \text{Re}(D)/m_t \\
K_{RR} &= 1 + 2\text{Re}(A) - \beta^2 \hat{s} \text{Re}(C)/m_t - \beta \hat{s} \text{Re}(D)/m_t \\
K_{LR} &= 1 + 2\text{Re}(A) + 2\beta \text{Re}(B) \\
K_{RL} &= 1 + 2\text{Re}(A) - 2\beta \text{Re}(B)
\end{aligned} \tag{9}$$

where $\beta = \sqrt{1 - 4m_t^2/\hat{s}}$. Figure 4 shows the K factors in the MSSM with $M_{H^+} = 180$ GeV for $\tan\beta = 1$ and 35, and in the SM with $M_{H^0} = 100$ GeV. The quark mixing from the CKM matrix is not included; therefore, CP is invariant and K_{LL} is equal to K_{RR} . The difference in K_{RL} and K_{LR} is generated by parity violating corrections.

The cross section of $p\bar{p} \rightarrow t\bar{t} + X$ is evaluated with the convolution of the subprocess cross section ($\hat{\sigma}(q\bar{q} \rightarrow t\bar{t})$) and parton distribution functions. The effects of parity violation appear as an asymmetry in the invariant mass distributions as well as in the integrated cross sections of $t_R\bar{t}_L$ and $t_L\bar{t}_R$. Let us define the differential asymmetry as

$$\begin{aligned}
\delta\mathcal{A}(M_{t\bar{t}}) &\equiv \frac{d\sigma_{RL}/dM_{t\bar{t}} - d\sigma_{LR}/dM_{t\bar{t}}}{d\sigma_{RL}/dM_{t\bar{t}} + d\sigma_{LR}/dM_{t\bar{t}}} \\
&= \frac{K_{RL} - K_{LR}}{K_{RL} + K_{LR}} \\
&= \frac{-2\beta \text{Re}(B)}{1 + 2\text{Re}(A)}
\end{aligned} \tag{10}$$

where the parton distribution functions are cancelled in the ratio. This differential asymmetry is presented in Figure 5 for the SM and the MSSM.

The form factor $B(k^2)$ is proportional to $\hat{s} = M_{tt}^2$; therefore, the differential asymmetry is enhanced at higher energy.

Since the helicity of the top quark has to be deduced from the energy distribution of the leptons in the W decays, it is more realistic to sum over the helicities of the \bar{t} and consider an integrated asymmetry in numbers of t_R and t_L . The number of observed $t\bar{t}$ will be reduced only by the branching ratio of $t \rightarrow W^+b \rightarrow l^+\nu_l b$. The integrated asymmetry is defined as

$$\begin{aligned}\mathcal{A} &\equiv \frac{N_R - N_L}{N_R + N_L} = \frac{\sigma_R - \sigma_L}{\sigma_R + \sigma_L} \\ N &= \mathcal{L}\sigma\end{aligned}\tag{11}$$

where $\sigma_R = \sigma_{RL} + \sigma_{RR}$, $\sigma_L = \sigma_{LR} + \sigma_{LL}$ and \mathcal{L} = the integrated luminosity. The statistical uncertainty ($\Delta\mathcal{A}$) and statistical significance (N_S) of the integrated asymmetry are

$$\begin{aligned}\Delta\mathcal{A} &= \frac{2\sqrt{N_R N_L}}{(N_R + N_L)^{3/2}} \sim \frac{1}{\sqrt{N_R + N_L}} \\ N_S &= \mathcal{A}/\Delta\mathcal{A}.\end{aligned}\tag{12}$$

To be conservative, we require $N_S \geq 4$ for an asymmetry to be possibly visible.

The difference ($\Delta\sigma$) and the total (σ) of the cross sections σ_R and σ_L with one loop SM weak corrections, as well as the integrated asymmetry (\mathcal{A}) and its statistical significance (N_S) are presented in Table I for an integrated luminosity of 10 fb^{-1} and 100 fb^{-1} . At $\sqrt{s} = 2 \text{ TeV}$, the asymmetry will not be visible even if $\mathcal{L} = 100 \text{ fb}^{-1}$. At $\sqrt{s} = 4 \text{ TeV}$, the asymmetry can become

larger than its uncertainty with $\mathcal{L} = 100 \text{ fb}^{-1}$. We find that requiring $M_{t\bar{t}} > 500 \text{ GeV}$ can efficiently enhance the asymmetry while only slightly increasing its uncertainty.

In the MSSM, the asymmetry can be enhanced if $\tan \beta > \sqrt{m_t/m_b}$. Table II shows the integrated asymmetry and its statistical significance in the MSSM for $M_{t\bar{t}} > 500 \text{ GeV}$. If $\tan \beta$ is close to one, the asymmetry \mathcal{A} from the MSSM weak corrections is smaller than that in the SM. For $10 > \tan \beta > 3$, the asymmetry generated from the MSSM weak corrections is very similar to that in the SM. At $\sqrt{s} = 2 \text{ TeV}$, the asymmetry \mathcal{A} can be larger than $\Delta\mathcal{A}$ for $\tan \beta > \sqrt{m_t/m_b}$ and $\mathcal{L} = 100 \text{ fb}^{-1}$. At $\sqrt{s} = 4 \text{ TeV}$, the parity violation signal is highly enhanced. With $\mathcal{L} = 100 \text{ fb}^{-1}$, this asymmetry might be visible for $M_{H^+} \leq 300 \text{ GeV}$ and $\tan \beta \geq m_t/m_b \sim 35$. Its statistical significance (N_S) can be larger than 4.8.

4. Conclusions

In the SM, the asymmetry of parity violation is almost independent of the Higgs boson mass. At $\sqrt{s} = 2 \text{ TeV}$, the asymmetry in N_R and N_L of $t\bar{t}$ is always smaller than its statistical uncertainty for an integrated luminosity of 10 fb^{-1} . It becomes slightly better with $\mathcal{L} = 100 \text{ fb}^{-1}$. At $\sqrt{s} = 4 \text{ TeV}$, the asymmetry is enhanced. However, it is still difficult to observe this asymmetry in the SM even with $\mathcal{L} = 100 \text{ fb}^{-1}$.

In the MSSM, the parity violation asymmetry depends mainly on $\tan \beta$ and M_{H^+} . It can be enhanced for $\tan \beta > \sqrt{m_t/m_b}$. The asymmetry in N_R

and N_L of $t\bar{t}$ might be visible at $\sqrt{s} = 2$ and $\mathcal{L} = 100 \text{ fb}^{-1}$ or at $\sqrt{s} = 4$ TeV and $\mathcal{L} = 10 \text{ fb}^{-1}$, if $\tan\beta \gg m_t/m_b$ and M_{H^+} close to m_t . At $\sqrt{s} = 4$ TeV, with $\mathcal{L} = 100 \text{ fb}^{-1}$, this asymmetry generated from the MSSM weak corrections might be visible for $M_{H^+} < 300 \text{ GeV}$ and $\tan\beta$ close to m_t/m_b .

The parity violation in top quark pair production might provide a good opportunity to study the parity violating interactions between the top quark and spin-0 or spin-1 particles. Because the parity violation signal is very small in the SM, any observation of large parity violation would indicate new physics.

Acknowledgements

I am grateful to Duane Dicus, Lynne Orr, Xerxes Tata, especially, Glenn Ladinsky and Chien-Peng Yuan for beneficial discussions, comments and instructions. This research was supported in part by the US Department of Energy grant DE-FG02-91ER40685.

References

- [1] The D0 group has reported that m_t is larger than 131 GeV in the Standard Model. S. Abachi et al. Phys. Rev. Lett. **72** (1994) 2138.
- [2] The CDF group has presented some evidence for the top quark with $m_t = 174 \pm 10^{+13}_{-12}$ GeV. F. Abe *et al.*, Phys. Rev. Lett. **73** (1994) 225; Phys. Rev. **D50** (1994) 2966.
- [3] P. Nason, S. Dawson and R.K. Ellis, Nucl. Phys. **B303** (1988) 607; **B327** (1989) 49.
- [4] W. Beenakker, H. Kuijf, W. van Neerven and J. Smith, Phys. Rev. **D40** (1989) 54; W. Beenakker, W.L. van Neerven, R. Meng, G.A. Schuler and J. Smith, Nucl. Phys. **B351** (1991) 507; R. Meng, G.A. Schuler, J. Smith and W.L. van Neerven, Nucl. Phys. **B339** (1990) 325.
- [5] F.A. Berends, J.B. Tausk, W.T. Giele, Phys. Rev. **D47** (1993) 2746.
- [6] E. Laenen, J. Smith, W.L. van Neerven, Phys. Lett. **B321** (1994) 254.
- [7] A. Stange and S. Willenbrock Phys. Rev. **D48** (1993) 2054.
- [8] C. Kao, G.A. Ladinsky, and C.-P. Yuan, FSU-HEP-930508, MSUHEP-93/04.
- [9] W. Beenakker, A. Denner, W. Hollik, R. Mertig and T. Sack, Nucl. Phys. **B411** (1994) 343.

- [10] C. Kao, G.A. Ladinsky, and C.-P. Yuan, FSU-HEP-940508, MSUHEP-94/04.
- [11] I. Bigi and H. Krasemann, Z. Phys. **C7** (1981) 127; J. Kühn, Acta Phys. Austriaca Suppl. **XXIV** (1982) 203; I. Bigi, Y. Dokshitzer, V. Khoze, J. Kühn and P. Zerwas, Phys. Lett. **B181** (1986) 157.
- [12] H.P. Nilles, Phys. Rep. **110** (1984) 1.
- [13] P. Nath, R. Arnowitt and A. Chamseddine, *Applied $N = 1$ Supergravity*, ICTP Series in Theoretical Physics, Vol. I, World Scientific (1984).
- [14] H.E. Haber and G.L. Kane, Phys. Rep. **117** (1985) 75.
- [15] J.F. Gunion, H.E. Haber, G.L. Kane and S. Dawson, *The Higgs Hunter's Guide*, Addison-Wesley, Redwood City, CA (1990).
- [16] X. Tata, in *The Standard Model and Beyond*, p. 304, edited by J. E. Kim, World Scientific (1991).
- [17] V. Barger, M. Berger, A. Stange and R. Phillips, Phys. Rev. **D45** (1992) 4128 .
- [18] H. Baer, M. Bisset, C. Kao and X. Tata, Phys. Rev. **D46** (1992) 1067; Phys. Rev. **D50** (1994) 316. H. Baer, M. Bisset, D. Dicus, C. Kao and X. Tata, Phys. Rev. **D47** (1993) 1062.

- [19] J.F. Gunion and L. Orr, Phys. Rev. **D46** (1992) 2052; J.F. Gunion, in *Perspectives on Higgs Physics*, ed. G. Kane, World Scientific Publishing (1992), and references therein.
- [20] Z. Kunszt and F. Zwirner, Nucl. Phys. **B385** (1992) 3.
- [21] J. Dai, J. F. Gunion and R. Vega, Phys. Lett. **B315** (1993) 355; UCD-94-7, (1994).
- [22] C. Hill and S. Parke, Phys. Rev. **D49** (1994) 4454.
- [23] E. Eichten and K. Lane, Phys. Lett. **B327** (1994) 129.
- [24] Y. Okada, M. Yamaguchi and T. Yanagida, Phys. Lett. **262B**, 54 (1991) and Prog. Theor. Phys. **85**, 1 (1991).
- [25] J. Ellis, G. Ridolfi and F. Zwirner, Phys. Lett. **257B**, (1991) 83.
- [26] H.E. Haber and R. Hempfling, Phys. Rev. Lett. **66**, 1815 (1991); H.E. Haber, in *Perspectives on Higgs Physics*, ed. G.L. Kane, World Scientific, Singapore, (1992), and references therein.
- [27] H.-L. Lai, J. Botts, J. Huston, J.G. Morfin, J.F. Owens, J.-W. Qiu, W.-K. Tung and H. Weerts, CTEQ-404 (1994).
- [28] G.L. Kane, G.A. Ladinsky and C.-P. Yuan, Phys. Rev. **D45** (1992) 124.

TABLE I. The difference ($\Delta\sigma$) and the total (σ) of cross sections σ_R and σ_L , and the asymmetry $\mathcal{A} = (N_R - N_L)/(N_R + N_L)$ generated by the SM weak corrections in $p\bar{p} \rightarrow t\bar{t} + X$, with $m_t = 170$ GeV, for (a) $\sqrt{s} = 2$ TeV and (b) $\sqrt{s} = 4$ TeV. At each energy, we consider both $M_{t\bar{t}} > 2m_t$, and $M_{t\bar{t}} > 500$ GeV. Also shown is the statistical significance (N_S) for $\mathcal{L} = 10$ fb $^{-1}$ and 100 fb $^{-1}$.

M_H (GeV)	$\Delta\sigma$ (fb)	σ (fb)	\mathcal{A} (%)	N_S (10 fb $^{-1}$)	N_S (100 fb $^{-1}$)
(a) $\sqrt{s} = 2$ TeV					
$M_{t\bar{t}} > 2m_t$					
100	3.76	4550	0.083	0.18	0.56
700	3.76	4510	0.083	0.18	0.56
$M_{t\bar{t}} > 500$ GeV					
100	3.00	845	0.36	0.33	1.0
700	3.00	858	0.35	0.32	1.0
(b) $\sqrt{s} = 4$ TeV					
$M_{t\bar{t}} > 2m_t$					
100	25.6	16240	0.16	0.63	2.0
700	25.6	16170	0.16	0.64	2.0
$M_{t\bar{t}} > 500$ GeV					
100	22.5	4860	0.46	1.0	3.2
700	22.5	4940	0.46	1.0	3.2

TABLE II. The difference and the total of cross sections σ_R and σ_L , and the asymmetry \mathcal{A} generated by the MSSM weak corrections, for $M_{t\bar{t}} > 500$ GeV as well as several values of M_{H^+} and $\tan\beta$. All notations and other parameters are the same as in Table I.

$\tan\beta$	$\Delta\sigma$ (fb)	σ (fb)	\mathcal{A} (%)	N_S (10 fb ⁻¹)	N_S (100 fb ⁻¹)
(a) $\sqrt{s} = 2$ TeV					
$M_{H^+} = 180$ GeV					
1	-1.11	835	-0.13	0.12	0.38
3	2.57	846	0.30	0.28	0.89
10	3.29	847	0.39	0.36	1.1
35	7.02	839	0.84	0.77	2.4
$M_{H^+} = 300$ GeV					
1	1.37	844	0.16	0.15	0.47
3	2.83	847	0.33	0.31	0.97
10	3.12	848	0.37	0.34	1.1
35	4.60	847	0.54	0.50	1.6
(b) $\sqrt{s} = 4$ TeV					
$M_{H^+} = 180$ GeV					
1	-4.08	4790	-0.085	0.19	0.59
3	19.7	4860	0.41	0.90	2.8
10	24.4	4870	0.50	1.1	3.5
35	48.5	4820	1.0	2.2	7.0
$M_{H^+} = 300$ GeV					
1	10.9	4840	0.23	0.50	1.6
3	21.3	4870	0.44	0.97	3.1
10	23.3	4880	0.48	1.1	3.3
35	33.8	4860	0.70	1.5	4.8
$M_{H^+} = 500$ GeV					
1	20.8	4860	0.43	0.94	3.0
3	22.3	4870	0.46	1.0	3.2
10	22.6	4880	0.46	1.0	3.2
35	24.2	4880	0.50	1.1	3.5

Figures

FIG. 1 The Feynman diagrams for weak corrections to (a) the top quark self energy and wave function renormalization and (b) the $gt\bar{t}$ vertex, in the SM and the MSSM. Both momenta p and q are flowing out of the vertex.

FIG. 2 The real part of the form factor $B(k^2)$ from diagrams with the Z , the G^+ , the W^+ , and the SM total, as a function of $M_{t\bar{t}}$ for $m_t = 170$ GeV.

FIG. 3 The real part of the form factor B_{MSSM} as a function of $M_{t\bar{t}}$, for (a) $M_{H^+} = 180$ GeV and (b) $M_{H^+} = 300$ GeV, with $\tan\beta = 1, 3, 10$, and 35. Also shown is real part of the form factor B_{SM} which is independent of the Higgs boson mass.

FIG. 4 The K -factor as a function of $M_{t\bar{t}}$, at various helicity states of $t\bar{t}$, (a) in the SM with $M_{H^0} = 100$ GeV, as well as in the MSSM with $M_{H^+} = 180$ GeV for (b) $\tan\beta = 1$, and (c) $\tan\beta = 35$. The first letter indicates the helicity of the t , the second letter indicates that of the \bar{t} .

FIG. 5 The asymmetry in the invariant mass distribution of $t\bar{t}$ as defined in Eq. 10, for (a) $M_{H^+} = 180$ GeV and (b) $M_{H^+} = 300$ GeV, with $\tan\beta = 1, 3, 10$, and 35. Also shown is the same asymmetry in the SM with $M_{H^0} = 100$ GeV (solid) and $M_{H^0} = 500$ GeV (dash).

This figure "fig1-1.png" is available in "png" format from:

<http://arXiv.org/ps/hep-ph/9411337v1>

This figure "fig1-2.png" is available in "png" format from:

<http://arXiv.org/ps/hep-ph/9411337v1>

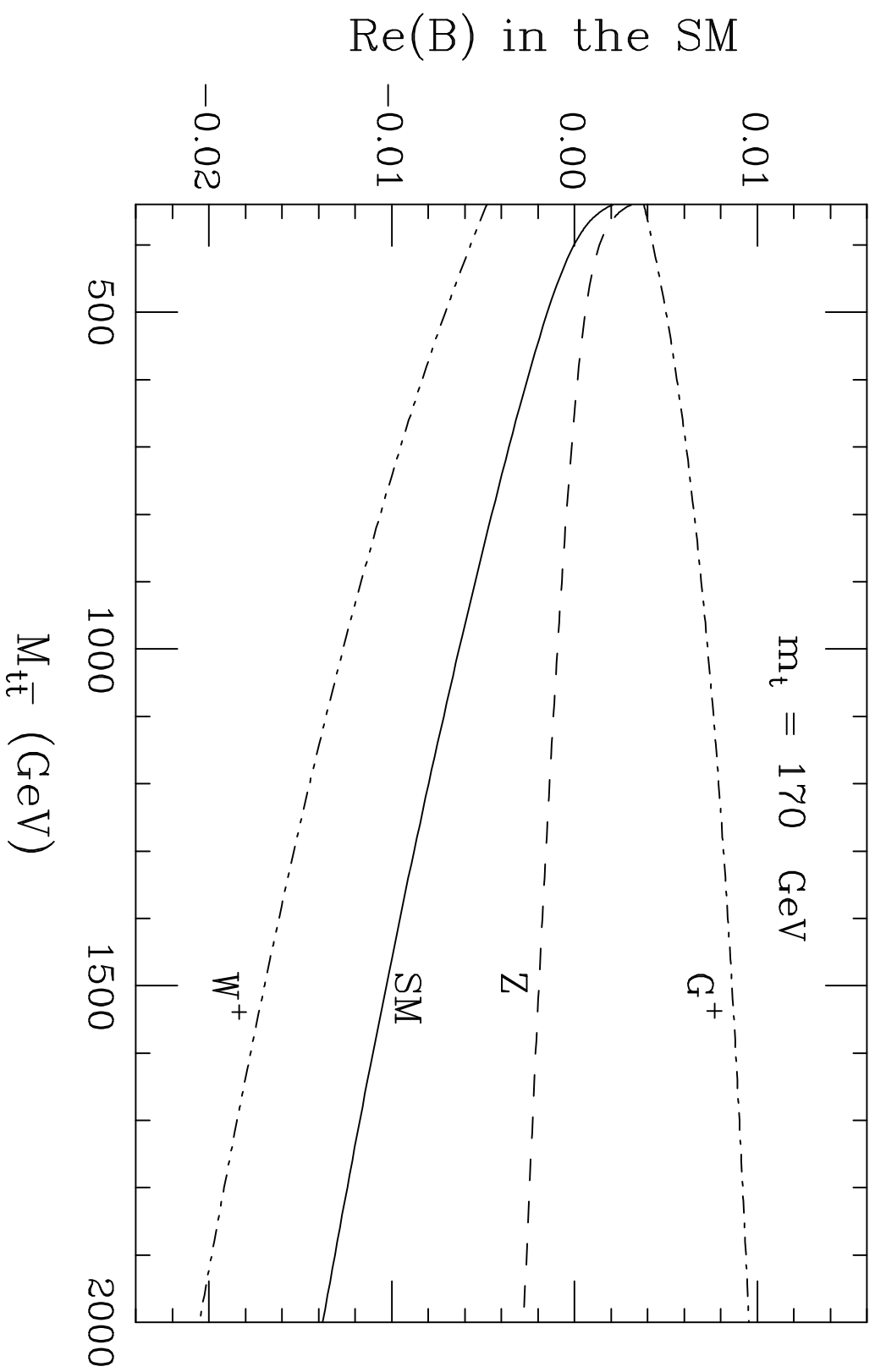


Figure 2

This figure "fig1-3.png" is available in "png" format from:

<http://arXiv.org/ps/hep-ph/9411337v1>

Re(B) in the MSSM

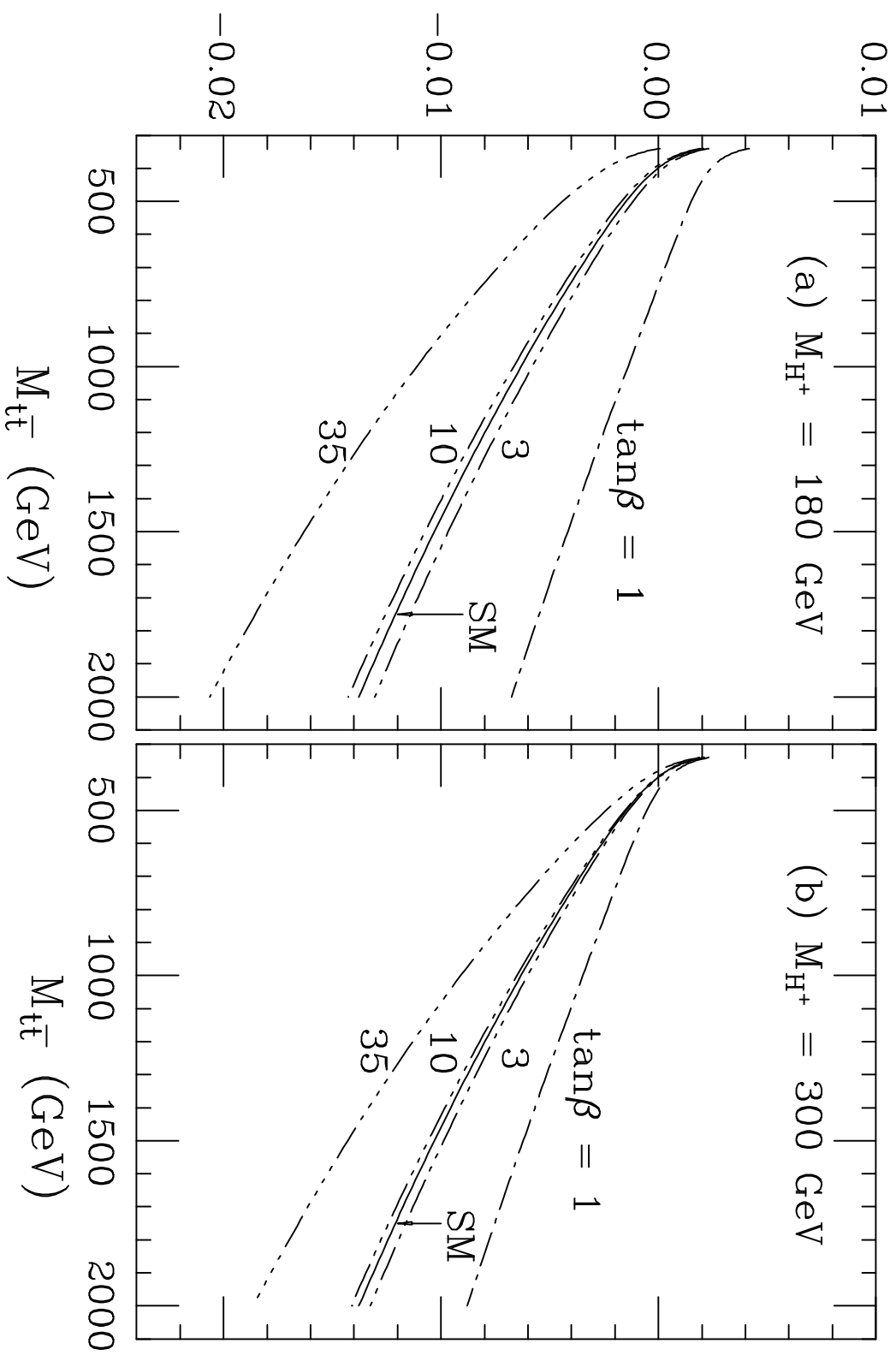


Figure 3

This figure "fig1-4.png" is available in "png" format from:

<http://arXiv.org/ps/hep-ph/9411337v1>

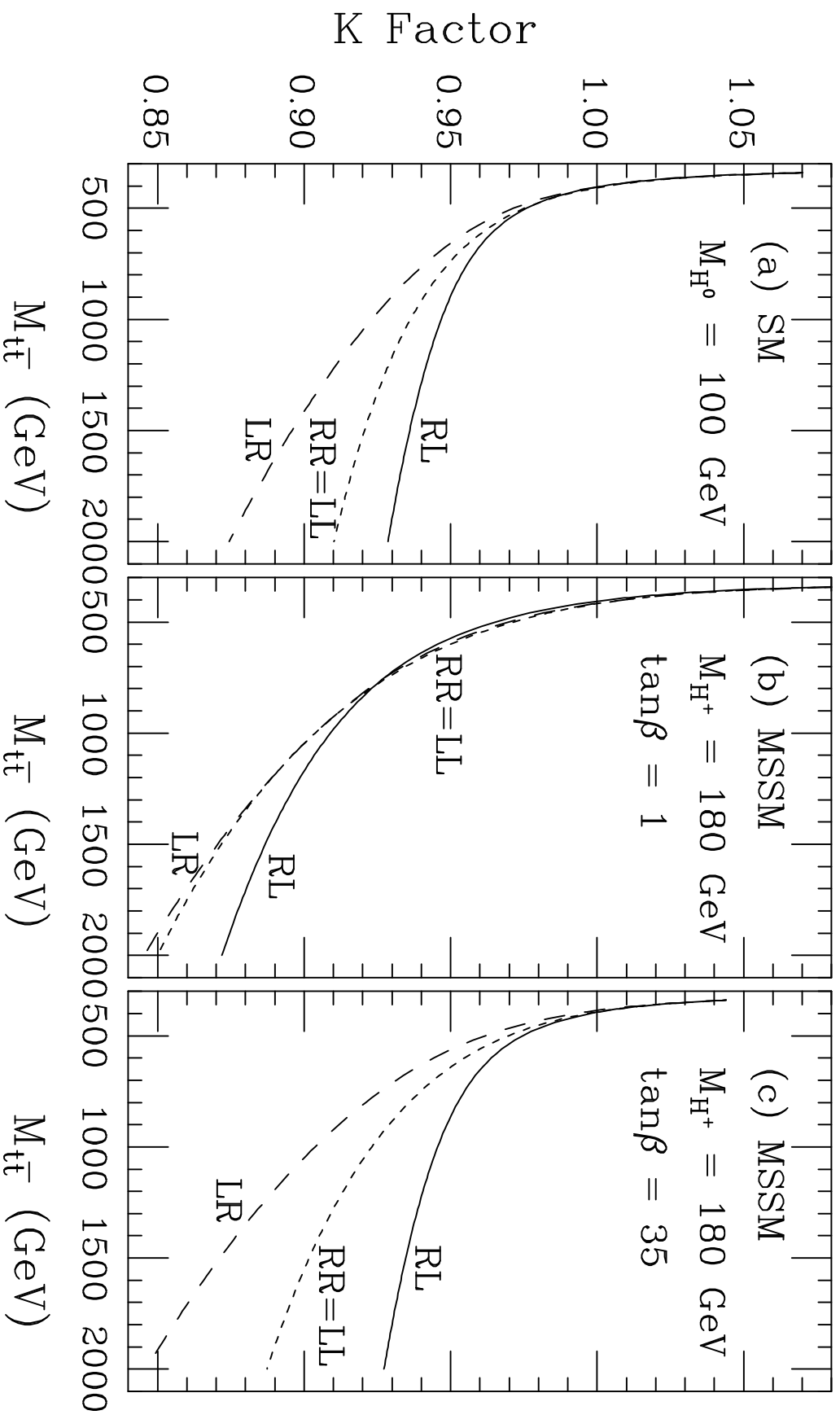


Figure 4

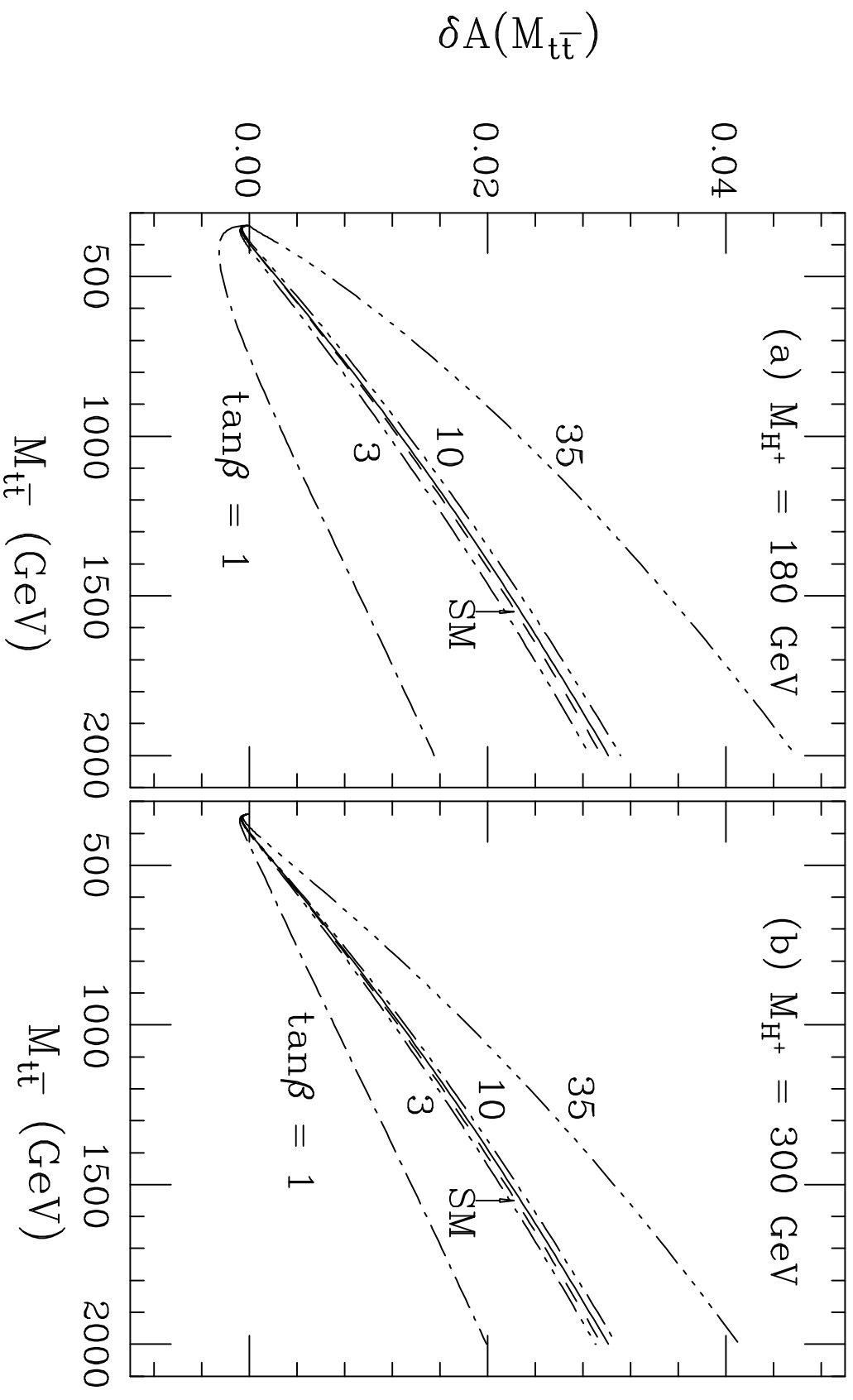


Figure 5